



## Data Article

# Dataset for the phase equilibria and PXRD studies of urea as a green thermodynamic inhibitor of sII gas hydrates



Anton P. Semenov<sup>a,b,\*</sup>, Yinghua Gong<sup>a,b</sup>, Rais I. Mendgaziev<sup>b</sup>,  
Andrey S. Stoporev<sup>a,b,c</sup>, Vladimir A. Vinokurov<sup>a,b</sup>, Tianduo Li<sup>a,\*</sup>

<sup>a</sup>Shandong Provincial Key Laboratory of Molecular Engineering, School of Chemistry and Chemical Engineering, Qilu University of Technology (Shandong Academy of Sciences), Jinan 250353, PR China

<sup>b</sup>Gubkin University, Department of Physical and Colloid Chemistry, 65, Leninsky prospekt, Building 1, Moscow 119991, Russian Federation

<sup>c</sup>Department of Petroleum Engineering, Kazan Federal University, Kremlevskaya str. 18, Kazan 420008, Russian Federation

## ARTICLE INFO

## Article history:

Received 2 April 2023

Accepted 5 June 2023

Available online 10 June 2023

Dataset link: [Raw data of gas hydrate equilibria and PXRD measurements in system C<sub>3</sub>H<sub>8</sub>/CH<sub>4</sub> – H<sub>2</sub>O – Urea \(Original data\)](#)

## Keywords:

sII gas hydrates

Methane-propane gas mixture

Thermodynamic hydrate inhibitor

Urea

Phase equilibria

Powder X-ray diffraction

## ABSTRACT

The equilibrium conditions of sII methane/propane hydrates have been experimentally determined for the C<sub>3</sub>H<sub>8</sub>/CH<sub>4</sub>-H<sub>2</sub>O-urea system. The equilibrium dissociation temperatures and pressures of sII hydrates span a wide *P,T*-range (266.7–293.9 K; 0.87–9.49 MPa) and were measured by varying the feed mass fraction of urea in solution from 0 to 50 mass%. The experimental points at feed urea concentration ≤ 40 mass% correspond to the V-L<sub>w</sub>-H equilibrium (gas-aqueous urea solution-gas hydrate). A four-phase V-L<sub>w</sub>-H-S<sub>u</sub> equilibrium (with an additional phase of solid urea) was observed because the solubility limit of urea in water was reached for all points at a feed mass fraction of 50 mass% and for one point at 40 mass% (266.93 K). Gas hydrate equilibria were measured using a high-pressure rig GHA350 under isochoric conditions with rapid fluid stirring and slow ramp heating of 0.1 K/h. Each measured point represents complete dissociation of the sII hydrate. The phase equilibrium data was compared with the literature reported for the C<sub>3</sub>H<sub>8</sub>/CH<sub>4</sub>-H<sub>2</sub>O and CH<sub>4</sub>-H<sub>2</sub>O-urea systems. A comprehensive analysis of the ther-

DOI of original article: [10.1016/j.cej.2021.132386](https://doi.org/10.1016/j.cej.2021.132386)

\* Corresponding authors.

E-mail addresses: [semenov.a@gubkin.ru](mailto:semenov.a@gubkin.ru) (A.P. Semenov), [litianduo@qlu.edu.cn](mailto:litianduo@qlu.edu.cn) (T. Li).

<https://doi.org/10.1016/j.dib.2023.109303>

2352-3409/© 2023 The Author(s). Published by Elsevier Inc. This is an open access article under the CC BY-NC-ND license (<http://creativecommons.org/licenses/by-nc-nd/4.0/>)

modynamic inhibition effect of urea to sII  $C_3H_8/CH_4$  hydrates on pressure and concentration of the inhibitor was carried out. The phase composition of the samples was analyzed by powder X-ray diffractometry at 173 K.

© 2023 The Author(s). Published by Elsevier Inc.

This is an open access article under the CC BY-NC-ND license (<http://creativecommons.org/licenses/by-nc-nd/4.0/>)

## Specifications Table

Subject	Chemistry
Specific subject area	Physical and Theoretical Chemistry
Type of data	Tables, figures
How the data were acquired	<p>The sII methane/propane hydrate equilibrium conditions were measured using a high-pressure rig GHA350 (PSL Systemtechnik, Germany) under isochoric conditions with ramp heating of 0.1 K/h coupled with vigorous fluid stirring at a rate of 10 revolutions per second. Each measured equilibrium point corresponds to the total disappearance of sII hydrate in the system upon linear heating. The high-pressure vessel GHA350 is 600 mL in volume. The quantity of the liquid phase (aqueous urea solution) fed into the autoclave was 500 g. The setup is equipped with temperature/pressure sensors. The fluids are mixed using a four-blade stirrer driven by a magnetic coupling (Premex, Switzerland) from an overhead device Hei-TORQUE 400 Precision (Heidolph, Germany). The temperature of the fluids in the autoclave changes according to the preset program by means of the Ministat 240 thermostat (Huber, Germany), which uses ethyl alcohol as a coolant. The coolant circulates inside the outer contour of the autoclave. The thermostat is controlled by a PC and a software package (WinGHA). This software enables the writing of script that control the operation of the apparatus and automatically record the readings of all the parameters on the PC.</p> <p>The analysis of the phase composition of the samples containing <math>C_3H_8/CH_4</math> hydrates was accomplished using a D8 Advance diffractometer (Bruker, Germany) equipped with a low-temperature device (Anton Paar, Austria). The diffractograms of pre-quenched samples at liquid nitrogen temperature were recorded under isothermal conditions at 173 K and atmospheric pressure.</p>
Data format	Raw and analyzed
Description of data collection	<p>Equilibrium temperatures and pressures of sII gas hydrates were determined for six feed mass fractions of urea in aqueous solution, comprising 0, 10, 20, 30, 40, and 50 mass%. The generated dataset consists of 39 equilibrium points and falls in the following <math>P,T</math>-region (266.7–293.9 K; 0.87–9.49 MPa). The phase composition was investigated for 4 samples of gas hydrates prepared from frozen aqueous urea solutions with feed mass fraction of 20 and 40 mass% at hydrate-forming gas pressures during synthesis of 1.5 and 6 MPa. In addition, a frozen aqueous urea solution (40 mass%) containing no methane/propane gas hydrates was studied. Diffractograms were recorded in the <math>2\theta</math> range from 5 to 42 degrees.</p>
Data source location	<p>Gubkin University, Department of Physical and Colloid Chemistry, Moscow, Russia. 55.692232°N, 37.55487°E</p>
Data accessibility	<p>Repository name: Mendeley Data Data identification number: <a href="https://data.mendeley.com/datasets/6mmwf3y864.1">10.17632/6mmwf3y864.1</a> Direct URL to data: <a href="https://data.mendeley.com/datasets/6mmwf3y864">https://data.mendeley.com/datasets/6mmwf3y864</a></p>
Related research article	<p>Y. Gong, R.I. Mendgaziev, W. Hu, Y. Li, Z. Li, A.S. Stoporev, A. Yu. Manakov, V.A. Vinokurov, T. Li, A.P. Semenov, Urea as a Green Thermodynamic Inhibitor of sII Gas Hydrates, Chem. Eng. J. (2022) 132386. <a href="https://doi.org/10.1016/j.cej.2021.132386">https://doi.org/10.1016/j.cej.2021.132386</a>. [1].</p>

## Value of the Data

- The phase equilibrium data can be used to predict the thermodynamic stability of sII gas hydrates across a vast range of temperatures, pressures, and urea concentrations.
- The data provide a comprehensive and accurate description of urea activity as a thermodynamic hydrate inhibitor for both mass% and mol% scales.
- The data allow the selection of the urea concentration in aqueous solution that provides a given thermodynamic inhibition effect for sII gas hydrates.
- The data can be used to develop new thermodynamic models and gas hydrate software or to modify existing ones.
- PXRD data provide new insights into the phase behavior of gas hydrates and urea in the  $C_3H_8/CH_4-H_2O$ -urea system.

## 1. Objective

The main objective of generation of this dataset was to systematically investigate urea as a promising and sustainable thermodynamic hydrate inhibitor (THI). To this end, we thoroughly studied the impact of urea on the phase equilibria of hydrates of a model methane/propane gas mixture (4.34  $C_3H_8$  / 95.66  $CH_4$  (mol%)), which mimics natural gas forming a hydrate of cubic structure II. In order to establish the role of urea in the formation of clathrate hydrates, we have also investigated the phase behavior in the  $C_3H_8/CH_4-H_2O$ -urea system by means of PXRD. The next goal of the work was to derive a correlation from hydrate dissociation data that would quantitatively describe urea anti-hydrate ability as a concentration- and pressure-dependent value. This correlation is necessary, because it allows a comparison of the thermodynamic inhibition effect of urea in systems with other hydrate-forming gases, as well as a comparison of urea with various THIs. The results of this study provide a physicochemical basis for the possible use of urea as a fairly efficient and environmentally benign inhibitor to prevent the formation of sII gas hydrates in the oil and gas industry.

## 2. Data Description

The raw log files with numerical data of the parameters (time, temperature, pressure, stirrer speed) recorded during the measurement of all hydrate equilibrium points are presented in the "Hydrate equilibrium ( $C_3H_8+CH_4$ -Urea- $H_2O$ )" archive (see <https://data.mendeley.com/datasets/6mmwf3y864>). This archive contains thirty nine files with the extension .xlsx; each file corresponds to a measurement of a single equilibrium point. The file name denotes the number of the equilibrium point (see points # in Table 1) and the mass fraction of urea in aqueous solution. For example, the file name "30% Urea\_point 24" provides the raw data for equilibrium point #24 where the urea concentration in the solution was 30 mass%. The files also contain the weighing results of  $H_2O$  and urea, from which the feed concentration of urea in water solution was calculated (see cells D1:H3).

The pressure and temperature-time curves in Fig. 1a illustrate the technique for measuring gas hydrate equilibrium conditions with the example of a 10 mass% aqueous urea solution. Panel b of Fig. 1 demonstrates the determination of the hydrate equilibrium point as the intersection of two linear segments of the  $P(T)$ -trajectory before and after the endpoint of hydrate dissociation. The numerical values of the gas hydrate dissociation conditions for  $C_3H_8/CH_4$ -Urea- $H_2O$  system (equilibrium temperature  $T$ , pressure  $P$ , and suppression of hydrate equilibrium temperature  $\Delta T_h$  at  $P$  value relative to system with pure  $H_2O$ ) are given in Table 1. In Fig. 2, the measured equilibrium points are plotted in  $P(T)$  coordinates with a logarithmic pressure axis. A comparison of our experimental data for system  $C_3H_8/CH_4$ -Urea- $H_2O$  (sII methane/propane hydrate) with literature data [2–4] for system  $CH_4$ -Urea- $H_2O$  (sI methane hydrate) and  $C_3H_8/CH_4-H_2O$

**Table 1**

Gas hydrate dissociation data for C<sub>3</sub>H<sub>8</sub>/CH<sub>4</sub>-Urea-H<sub>2</sub>O system (equilibrium temperature *T*, pressure *P*, and suppression of hydrate equilibrium temperature  $\Delta T_h$  at *P* value relative to system with pure H<sub>2</sub>O (sample #1)); heating rate near the endpoint of C<sub>3</sub>H<sub>8</sub>/CH<sub>4</sub> hydrate decomposition was 0.1 K/h except for point #18 (0.5 K/h)

Sample #	Initial urea concentration in aqueous solution, mass% <sup>a</sup> (mol%)	Point #	<i>T</i> , K <sup>b</sup>	<i>P</i> , MPa <sup>c</sup>	$\Delta T_h$ , K
1	0	1	276.34	1.00	0
		2	276.37	1.01	0
		3	279.41	1.43	0
		4	282.71	2.10	0
		5	285.57	2.95	0
		6	287.87	3.93	0
		7	289.52	4.90	0
		8	290.72	5.82	0
		9	292.04	7.04	0
		10	292.89	7.98	0
		11	293.91	9.57	0
2	10.00 (3.23)	12	272.92	0.87	2.15
		13	279.98	1.95	2.13
		14	285.42	3.79	2.14
		15	289.78	6.87	2.11
		16	291.74	9.49	2.13
3	20.00 (6.98)	17	270.93	0.88	4.25
		18	270.96 <sup>d</sup>	0.88 <sup>d</sup>	4.28 <sup>d</sup>
		19	277.88	1.98	4.37
		20	283.48	3.96	4.44
		21	287.43	6.93	4.52
		22	289.18	9.37	4.63
4	30.00 (11.39)	23	268.25	0.87	6.82
		24	268.24	0.86	6.76
		25	275.27	1.96	6.87
		26	280.76	3.92	7.08
		27	284.71	6.90	7.21
		28	286.37	9.38	7.44
		29	266.93 <sup>e</sup>	0.90 <sup>e</sup>	8.45
5	40.00 (16.66)	30	272.58	2.02	9.82
		31	277.72	3.95	10.17
		32	281.38	6.93	10.57
		33	282.98	9.47	10.89
6	50.00 (23.07)	34	266.68 <sup>e</sup>	0.95 <sup>e</sup>	9.20
		35	271.78 <sup>e</sup>	1.90 <sup>e</sup>	10.10
		36	276.25 <sup>e</sup>	3.69 <sup>e</sup>	11.10
		37	276.53 <sup>e</sup>	3.83 <sup>e</sup>	11.13
		38	279.42 <sup>e</sup>	6.65 <sup>e</sup>	12.25
		39	280.75 <sup>e</sup>	9.20 <sup>e</sup>	12.95

<sup>a</sup> Expanded uncertainty of urea mass fraction is 0.02 mass% (*k* = 2)

<sup>b</sup> Expanded uncertainty is 0.1 K (*k* = 2)

<sup>c</sup> Expanded uncertainty is 0.02 MPa (*k* = 2)

<sup>d</sup> Heating rate is 0.5 K/h

<sup>e</sup> Solid phase of urea is present in the system (four phases in equilibrium V-L<sub>w</sub>-H-S<sub>urea</sub>) making the urea equilibrium concentration in solution less than the initial one (see Section 3.1 and Table S1 in Supplementary of the original research paper [1])

(with close propane mole fractions in the gas of 4.3% [5], 3.1%, 4.9% [6], 4.4% [7], and 4.0% [8]) is shown in Fig. 3.

The three-dimensional plots of the variation of the thermodynamic inhibition effect of sII C<sub>3</sub>H<sub>8</sub>/CH<sub>4</sub> hydrate as a function of the equilibrium urea concentration in the water solution (mass% and mol%) and pressure are shown in Fig. 4. The numerical values of the coefficients for approximating surfaces of Fig. 4 (eq. 4 from ref. [9]) can be found in Table 2. Fig. 5 shows

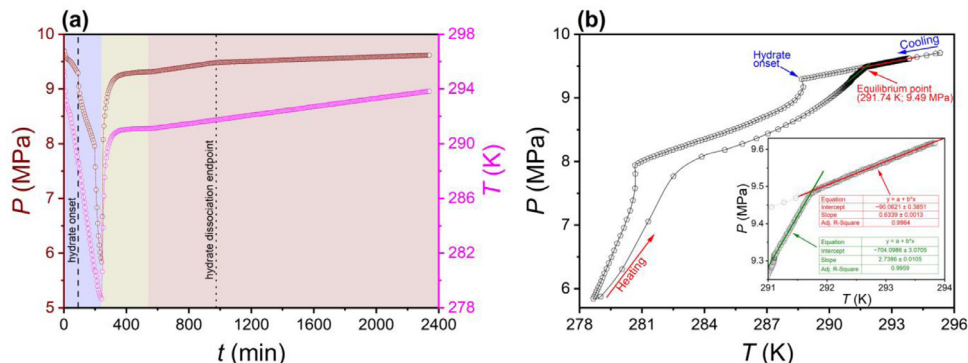


**Fig. 1.** (a) Pressure and temperature-time curves illustrating the technique for measuring gas hydrate equilibrium conditions with the example of a 10 mass% aqueous urea solution; blue, yellow, and brown areas refer to the cooling stage of 5 K/h (hydrate formation), 1st stage heating (decomposition of a major part of the gas hydrate with reaching the  $T$  and  $P$  plateau), and 0.1 K/h ramp heating, respectively; dashed and dotted lines indicate the times of gas hydrate occurrence in the system and complete dissociation; (b)  $P(T)$ -trajectory represents the determination of the hydrate equilibrium point as the intersection of two linear segments before and after the endpoint of hydrate dissociation.

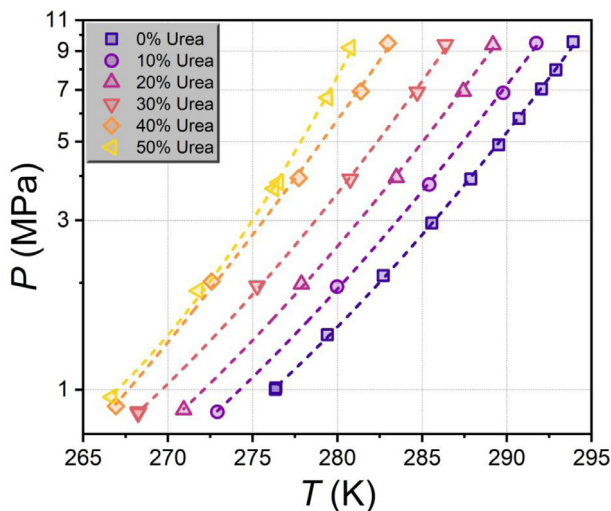


**Fig. 2.** Measured values (symbols) of equilibrium temperatures and pressures for the system  $C_3H_8/CH_4$ -Urea- $H_2O$  at urea concentration in aqueous solution 0–50 mass% (feed composition) and approximation results (dashed lines) of experimental points by the empirical equation  $P = \exp(A + B/T + C \ln T)$ ; approximation parameters are given in the original paper (Table S3 in the Supplementary of ref. [11])

the difference between experimental  $\Delta T_{h,exp}$  and calculated  $\Delta T_{h,fit}$  values as a function of the independent variables (pressure and equilibrium urea concentration in solution). Numerical values of difference  $\Delta T_{h,exp} - \Delta T_{h,fit}$  are given in Tables 3 and 4 for mass and mole fractions of urea, respectively. Fig. 6 depicts the 3D comparison of the thermodynamic inhibition effect as a function of the urea feed concentration in the water solution (mass%) for sII  $C_3H_8/CH_4$  hydrate (our data) and sI  $CH_4$  hydrate (experimental data [2,3]). The calculation of the methane hydrate equilibrium temperature suppression of the experimental points [2] was based on our numerical data on the gas-water-hydrate equilibrium for the system  $CH_4$ - $H_2O$  [9] and on data of Melnikov et al. [10] on the metastable equilibrium gas-supercooled water-hydrate.

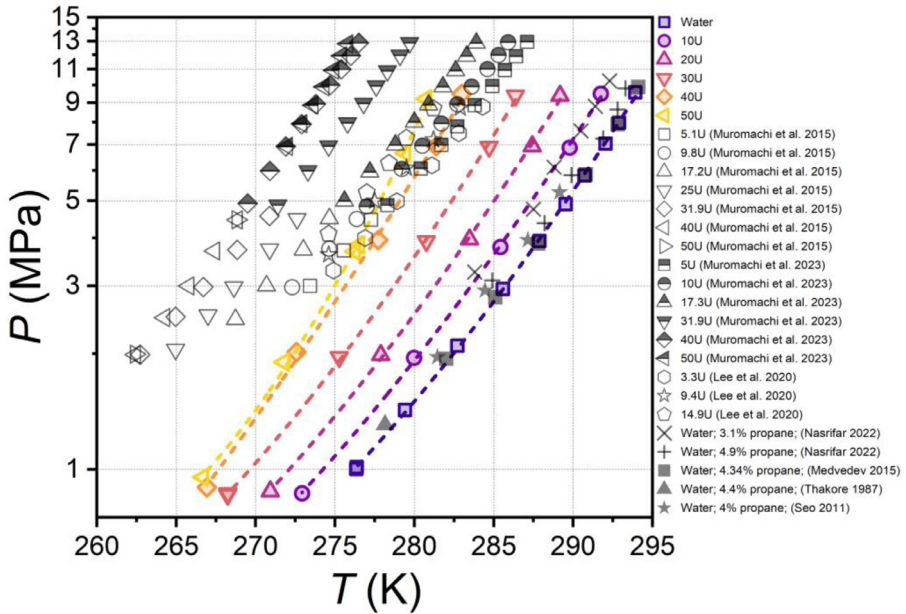


**Fig. 3.** Comparison of experimental data for system  $C_3H_8/CH_4$ -Urea- $H_2O$  (sII hydrate) with literature data [2–4] for system  $CH_4$ -Urea- $H_2O$  (sI hydrate) and  $C_3H_8/CH_4$ - $H_2O$  (with close propane mol fractions in gas of 4.3% [5], 3.1% and 4.9% [6], 4.4% [7], 4.0% [8]; sII hydrates); colored markers – our data, colored dashed lines – approximations based on our data (see caption of Fig. 2), black-edge markers – literature data; number before U in the sample name means feed mass percentage of urea in water solution, water sample means 0% urea

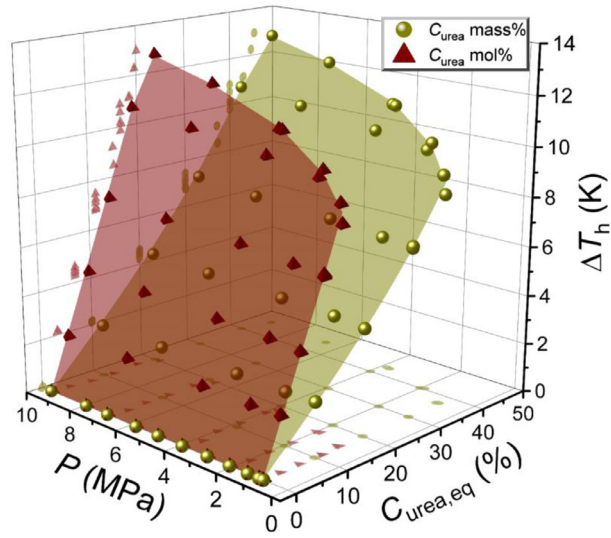


**Fig. 4.** The three-dimensional diagrams representing the variation of the thermodynamic inhibition effect of sII  $C_3H_8/CH_4$  hydrate as a function of the urea equilibrium concentration in the water solution (mass% and mol%) and pressure, markers – experimental quantities of  $\Delta T_h$  (see Table 1), surfaces are approximations by function 4 from ref. [9] (coefficients are in Table 2)

**Table 2**

The coefficients of empirical correlation (eq. 4 in paper [9]) of thermodynamic inhibition effect of urea  $\Delta T_h$  in the system  $C_3H_8/CH_4$ -Urea- $H_2O$  as a function of pressure (0.9–9.5 MPa) and equilibrium urea percentage of solution (0–45.7 mass% or 0–20.1 mol%)

Coefficient	mass% scale	mol% scale
$b_1$	2430.4133758	262.0247445
$b_2$	-2.9809667	-4.6099977
$b_3$	0.469481	0.2566218
$b_4$	-0.0020852	-0.0053194
$b_5$	$8.2512408 \cdot 10^{-5}$	0.0025033
$b_6$	$9.871456 \cdot 10^{-7}$	$2.9465706 \cdot 10^{-5}$
$b_7$	$5.6717097 \cdot 10^{-9}$	$2.2192651 \cdot 10^{-7}$
Adjusted $R^2$	0.9993	0.9993
Average absolute deviation (K)	0.08	0.08
Average absolute relative deviation (%)	1.56	1.56

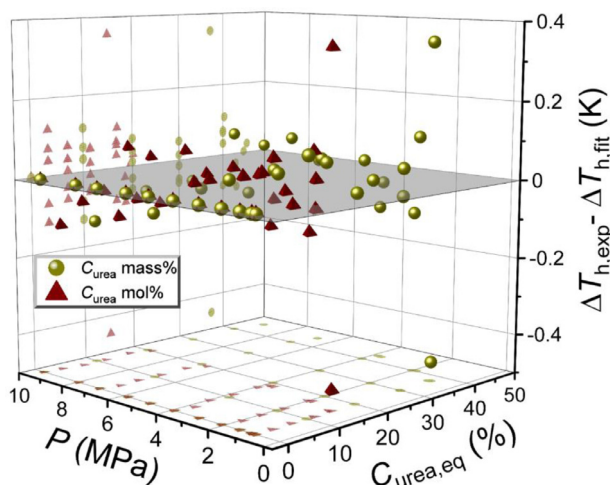


**Fig. 5.** The three-dimensional graph of  $\Delta T_h$  fitting residuals (numerical values are given in Tables 3 and 4) as a function of the independent variables (pressure and equilibrium solution concentration of urea in mass% and mol%)

The archive “PXRD analysis ( $C_3H_8+CH_4$ -Urea- $H_2O$ )” contains the raw powder X-ray diffraction data of gas hydrate samples prepared from frozen aqueous solutions of urea. Diffractograms were recorded for five samples. Two of them were collected for the samples obtained from 20 mass% aqueous urea solution (samples 1 and 2). For samples 1 and 2, the pressure of the hydrate-forming gas during the synthesis was 1.5 and 6 MPa, respectively. Two diffractograms were acquired for the samples synthesized from 40 mass% urea solution (samples 3 and 4). For samples 3 and 4, the gas pressure during hydrate synthesis was 1.5 and 6 MPa, respectively. A diffraction pattern was obtained for a frozen 40 mass% urea solution (sample 5) without methane/propane hydrates. There is a separate file containing numerical values of  $2\theta$  (degree) and signal intensity (a.u.) for each sample. Table 5 tabulates PXRD data for methane/propane hydrate samples obtained from 20 and 40 mass% urea solutions.

**Table 3**

Surface fitting data by empirical function 4 from ref. [9] of the gas hydrate equilibrium temperature suppression  $\Delta T_h$  versus the equilibrium urea mass fraction in water solution and pressure in system  $C_3H_8/CH_4$ -Urea- $H_2O$

Equilibrium urea mass fraction in solution, mass%	$P$ , MPa	$\Delta T_h$ experiment, K	$\Delta T_h$ fit, K	Residuals of $\Delta T_h$ (experiment-fit), K
0	0.87	0	0	0
0	1.00	0	0	0
0	1.01	0	0	0
0	1.43	0	0	0
0	2.10	0	0	0
0	2.95	0	0	0
0	3.93	0	0	0
0	4.90	0	0	0
0	5.82	0	0	0
0	7.04	0	0	0
0	7.98	0	0	0
0	9.57	0	0	0
10.00	0.87	2.15	2.04	0.11
10.00	1.95	2.13	2.07	0.06
10.00	3.79	2.14	2.11	0.03
10.00	6.87	2.11	2.19	-0.08
10.00	9.49	2.13	2.26	-0.13
20.00	0.88	4.25	4.24	0.01
20.00	1.98	4.37	4.30	0.07
20.00	3.96	4.44	4.40	0.04
20.00	6.93	4.52	4.56	-0.03
20.00	9.37	4.63	4.69	-0.06
30.00	0.86	6.82	6.77	0.05
30.00	0.87	6.76	6.77	-0.02
30.00	1.96	6.87	6.86	0.01
30.00	3.92	7.08	7.02	0.05
30.00	6.90	7.21	7.28	-0.06
30.00	9.38	7.44	7.49	-0.05
37.27 <sup>a</sup>	0.90	8.45	8.90	-0.45
40.00	2.02	9.82	9.90	-0.09
40.00	3.95	10.17	10.13	0.03
40.00	6.93	10.57	10.50	0.07
40.00	9.47	10.89	10.82	0.06
37.09 <sup>b</sup>	0.95	9.20	8.85	0.35
40.30 <sup>b</sup>	1.90	10.10	9.99	0.11
42.98 <sup>b</sup>	3.69	11.10	11.13	-0.03
43.18 <sup>b</sup>	3.83	11.13	11.22	-0.10
44.90 <sup>b</sup>	6.65	12.25	12.25	0.00
45.67 <sup>b</sup>	9.20	12.95	12.93	0.03

<sup>a,b</sup> The equilibrium concentration of urea in aqueous solution is less than the feed concentration (<sup>a</sup>40 and <sup>b</sup>50 mass%) due to the urea solubility limit; the equilibrium concentration was calculated from urea solubility measured at excess gas pressure (see Section 3.1 and Table S1 in Supplementary of the original research paper [11])

**Table 4**

Surface fitting data by empirical function 4 from ref. [9] of the gas hydrate equilibrium temperature suppression  $\Delta T_h$  versus equilibrium urea mol fraction in water solution and pressure in system  $C_3H_8/CH_4$ -Urea- $H_2O$

Equilibrium urea mol fraction in solution, mol%	$P$ , MPa	$\Delta T_h$ experiment, K	$K\Delta T_h$ fit, K	Residuals of $\Delta T_h$ (experiment-fit), K
0	0.87	0	0	0
0	1.00	0	0	0
0	1.01	0	0	0
0	1.43	0	0	0
0	2.10	0	0	0
0	2.95	0	0	0
0	3.93	0	0	0
0	4.90	0	0	0
0	5.82	0	0	0
0	7.04	0	0	0
0	7.98	0	0	0
0	9.57	0	0	0
3.23	0.87	2.15	2.04	0.12
3.23	1.95	2.13	2.06	0.07
3.23	3.79	2.14	2.11	0.04
3.23	6.87	2.11	2.19	-0.08
3.23	9.49	2.13	2.26	-0.12
6.98	0.88	4.25	4.24	0.01
6.98	1.98	4.37	4.30	0.07
6.98	3.96	4.44	4.40	0.04
6.98	6.93	4.52	4.56	-0.04
6.98	9.37	4.63	4.70	-0.07
11.39	0.86	6.82	6.77	0.06
11.39	0.87	6.76	6.77	-0.01
11.39	1.96	6.87	6.86	0.02
11.39	3.92	7.08	7.02	0.06
11.39	6.90	7.21	7.27	-0.06
11.39	9.38	7.44	7.49	-0.05
15.12 <sup>a</sup>	0.90	8.45	8.90	-0.45
16.66	2.02	9.82	9.90	-0.09
16.66	3.95	10.17	10.13	0.03
16.66	6.93	10.57	10.50	0.07
16.66	9.47	10.89	10.83	0.06
15.03 <sup>b</sup>	0.95	9.20	8.85	0.35
16.84 <sup>b</sup>	1.90	10.10	9.99	0.11
18.44 <sup>b</sup>	3.69	11.10	11.13	-0.03
18.56 <sup>b</sup>	3.83	11.13	11.22	-0.10
19.64 <sup>b</sup>	6.65	12.25	12.25	0.01
20.14 <sup>b</sup>	9.20	12.95	12.93	0.03

<sup>a,b</sup> The equilibrium concentration of urea in aqueous solution is less than the feed concentration (<sup>a</sup>16.66 and <sup>b</sup>23.07 mol%) due to the urea solubility limit; the equilibrium concentration was calculated from urea solubility measured at excess gas pressure (see Section 3.1 and Table S1 in Supplementary of the original research paper [1])

**Table 5**

Powder X-ray diffraction data for a frozen sample of aqueous urea solution and C<sub>3</sub>H<sub>8</sub>/CH<sub>4</sub> hydrate samples synthesized from aqueous urea solutions; the diffractograms were recorded at a temperature of 173 K; see the Experimental design, materials, and methods section for more details

20 mass% urea; 1.5 MPa	20 mass% urea; 6.0 MPa	40 mass% urea; 1.5 MPa	40 mass% urea; 6.0 MPa	40 mass% urea; 40 mass% urea	Calculated data on sII C <sub>3</sub> H <sub>8</sub> /CH <sub>4</sub> hydrate <sup>a</sup> , ice Ih <sup>b</sup> , and U <sup>c</sup>	
$2\theta_{\text{exp}} / ^\circ$	$2\theta_{\text{calc}} / ^\circ$	hkl/phase				
8.938	8.916	8.946	8.903	–	8.917	111/sII
14.592	14.569	14.595	14.553	–	14.586	022/sII
17.121	17.098	17.116	17.099	–	17.121	113/sII
17.878	17.853	17.883	17.857	–	17.888	222/sII
–	–	18.927	18.903	18.926	18.905	001/U
20.661	20.645	20.660	20.647	–	20.684	004/sII
22.462	22.463	22.470	22.456	22.466	22.460	110/U
–	–	–	–	–	22.563	313/sII
22.792	–	22.804	–	22.800	22.798	010/Ih
24.282	–	24.267	–	24.284	24.271	002/Ih
24.775	24.751	24.765	24.743	24.763	24.752	101/U
25.372	25.347	25.370	25.347	–	25.403	422/sII
25.876	–	25.866	–	25.880	25.871	011/Ih
26.935	26.913	26.933	26.909	–	26.972	511/333/sII
29.377	29.349	29.382	26.358	–	29.415	044/sII
–	–	29.487	29.475	29.518	29.518	111/U
30.748	30.720	30.744	30.722	–	30.795	513/sII
31.189	31.165	31.191	31.165	–	31.243	244/sII
31.967	31.929	31.953	31.944	31.975	31.974	020/U
32.923	32.899	32.917	32.889	–	32.980	602/sII
33.531	–	33.544	–	33.531	33.541	012/Ih
34.164	34.152	34.171	34.141	–	34.231	533/sII
–	–	–	–	–	34.639	226/sII
35.844	35.846	35.846	35.846	35.842	35.869	210/U
–	–	–	–	–	36.232	444/sII
–	–	–	–	–	37.388	117/155/sII
37.352	37.338	37.386	37.361	37.405	37.407	201/U
–	–	38.366	38.336	38.320	38.351	002/U
–	–	–	–	–	39.249	246/sII
40.036	–	40.014	–	40.024	40.036	110/Ih
–	40.213	40.274	40.216	–	40.331	137/535/sII
40.828	40.818	40.845	40.818	40.844	40.851	121/U
41.737	41.719	41.743	41.716	41.761	41.729	012/U

<sup>a</sup> Fd $\bar{3}$ m cubic structure II

<sup>b</sup> P6<sub>3</sub>/mmc hexagonal ice

<sup>c</sup> P4<sub>2</sub>1m tetragonal phase I urea

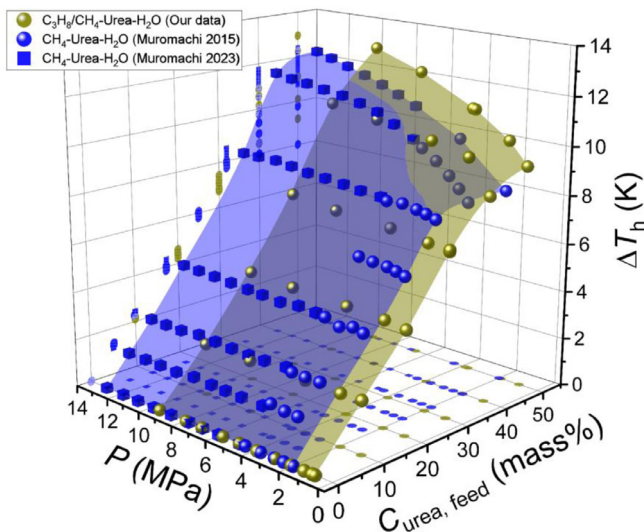


**Fig. 6.** Comparison of the thermodynamic inhibition impact as a function of the urea feed concentration in the water solution (mass%) for all  $C_3H_8/CH_4$  hydrate (our data) and all  $CH_4$  hydrate (experimental data from ref. [2,3]); symbols are experimental quantities, smooth surfaces are shown as a guide to the eye and interpolate experimental points for  $C_3H_8/CH_4$ -Urea- $H_2O$  and  $CH_4$ -Urea- $H_2O$  systems

### 3. Experimental Design, Materials, and Methods

The starting components for the model gas mixture (4.34  $C_3H_8$  / 95.66  $CH_4$  (mol%)) were high-purity methane gas (>99.99 vol%, Moscow Gas Processing Plant, Russia) and liquefied propane (>99.95 mass%, Linde Gas Rus, Moscow, Russia). The model gas mixture was prepared gravimetrically using equipment and technique as described at length in the original paper [1]. The propane mole fraction value of 4.34 % in the gas mixture was confirmed by gas chromatography. The estimated uncertainty (Type B) of the propane mole fraction based on the measured component masses ( $C_3H_8$  and  $CH_4$ ) and the metrological characteristics of the balance is  $\pm 0.06$  mol%. Urea with purity >99.5 mass% was supplied by Sigma Aldrich (USA). Aqueous solutions were prepared from 18.2  $M\Omega \cdot cm$  deionized water produced by an in-house Simplicity UV system (Millipore, USA). Aqueous solutions were prepared by mixing in a 1 L glass flask the components weighed to 0.001 g using a PA413C balance (Ohaus Pioneer, USA) with a maximum error of  $\pm 0.01$  g.

The GHA350 is configured with a Pt100 platinum resistance thermometer (accuracy  $\pm 0.1$  K) and a pressure sensor (accuracy  $\pm 0.02$  MPa). To ensure reliable results, the pressure and temperature sensors have been calibrated against reference instruments; a detailed description of the procedure can be found elsewhere [1]. A set of equipment including a Hei-TORQUE 400 Precision overhead motor (Heidolph, Germany), a magnetic coupling (Premex, Switzerland), and a four-blade propeller serves to intensively stir the test medium in the autoclave, which is a critical factor to ensure reliable hydrate equilibrium data [11]. To maintain the set temperature in the autoclave, a Ministat 240 thermostat (Huber, Germany) is employed, which uses ethanol as a coolant and circulates it in the outer jacket of the GHA350 autoclave. The Ministat 240 has a coolant temperature stability of no worse than  $\pm 0.02$  K.

The internal volume of the autoclave was thoroughly cleaned with deionized water and dried with compressed air before each series of experiments. A 500 g aqueous urea solution was filled into the GHA350 high-pressure vessel having the volume of 600 mL. The air was evacuated by purging the free volume three times with a methane-propane gas mixture. The autoclave was then filled with a gas mixture to the specified initial pressure and the experiment was

started (Fig. 1). Gas hydrate dissociation conditions were defined by the ramp heating technique. Successful implementation of this technique to measure hydrate equilibria has been previously described for a number of systems with THIs including, methanol [12–14], mono- and diethylene glycol [12,13], and DMSO [15,16]. The hydrate dissociation endpoint was detected by an acute change in the slope of the  $P(T)$ -trajectory at 0.1 K/h heating, as shown in Fig. 1b.

Powder X-ray diffraction was employed to analyze the phase composition of hydrate samples obtained from frozen aqueous solutions containing 20 and 40 mass% urea. A D8 Advance diffractometer (Bruker, Germany) integrated with a low temperature instrument (Anton Paar, Austria) was employed for sample analysis. An aqueous urea solution was frozen at 77 K (liquid  $N_2$ ), ground in a mortar, and the resulting powder was placed in an autoclave at 253 K. After flushing the empty volume with a gas mixture, a pressure of 1.5 or 6 MPa was set in the autoclave. The autoclave temperature was then increased to 274 K and the hydrate was synthesized for 12 h. The autoclave was then cooled to 77 K and the sample was retrieved and ground at this temperature. The resulting powder was compacted into a sample holder pre-cooled to 173 K. Diffractograms were registered at 173 K by  $2\theta$  scanning from 5 to 42 degrees. Hexagonal ice and tetragonal phase I urea reflections were used as an internal standard. Thus, the positions of the hydrate reflections were corrected, considering the shift in the ice/urea peaks positions. The calculated values ( $2\theta_{calc}$ ) were determined based on the literature data on unit cell parameters [17–19].

## Ethics Statements

The studies described in the manuscript adhered to Ethics in publishing standards (<https://www.elsevier.com/journals/data-in-brief/2352-3409/guide-for-authors>) and did not involve human or animal subjects.

## Declaration of Competing Interests

The authors declare that they have no known competing financial interests or personal relationships that could have appeared to influence the work reported in this paper.

## Data Availability

Raw data of gas hydrate equilibria and PXRD measurements in system C3H8/CH4 – H2O – Urea (Original data) (Mendeley Data).

## CRedit Author Statement

**Anton P. Semenov:** Data curation, Visualization, Validation, Conceptualization, Formal analysis, Methodology, Writing – original draft, Writing – review & editing; **Yinghua Gong:** Investigation; **Rais I. Mendgaziev:** Investigation, Data curation; **Andrey S. Stoporev:** Methodology, Investigation, Visualization, Formal analysis, Writing – original draft, Writing – review & editing; **Vladimir A. Vinokurov:** Resources, Supervision, Project administration; **Tianduo Li:** Resources, Supervision, Funding acquisition.

## Acknowledgments

This work was supported by the Program for Scientific Research Innovation Team in Colleges and Universities of Shandong Province of Qilu University of Technology (Shandong Academy of Sciences).

## References

- [1] Y. Gong, R.I. Mendgaziev, W. Hu, Y. Li, Z. Li, A.S. Stoporev, A. Yu. Manakov, V.A. Vinokurov, T. Li, A.P. Semenov, Urea as a green thermodynamic inhibitor of sII gas hydrates, *Chem. Eng. J.* (2022) 132386, doi:[10.1016/j.ccej.2021.132386](https://doi.org/10.1016/j.ccej.2021.132386).
- [2] S. Muromachi, T. Abe, T. Maekawa, Y. Yamamoto, Phase equilibrium for clathrate hydrate formed in methane+water+urea system, *Fluid Phase Equilib.* 398 (2015) 1–4, doi:[10.1016/j.fluid.2015.04.007](https://doi.org/10.1016/j.fluid.2015.04.007).
- [3] S. Muromachi, K. Suzuki, N. Tenma, Phase equilibrium data for clathrate hydrates formed in the systems of urea + (methane or carbon dioxide) + water, *Fluid Phase Equilib.* 568 (2023) 113743, doi:[10.1016/j.fluid.2023.113743](https://doi.org/10.1016/j.fluid.2023.113743).
- [4] D. Lee, W. Go, J. Oh, J. Lee, I. Jo, K.-S. Kim, Y. Seo, Thermodynamic inhibition effects of an ionic liquid (choline chloride), a naturally derived substance (urea), and their mixture (deep eutectic solvent) on CH<sub>4</sub> hydrates, *Chem. Eng. J.* 399 (2020) 125830, doi:[10.1016/j.ccej.2020.125830](https://doi.org/10.1016/j.ccej.2020.125830).
- [5] V.I. Medvedev, P.A. Gushchin, V.S. Yakushev, A.P. Semenov, Study of the effect of the degree of overcooling during the formation of hydrates of a methane-propane gas mixture on the equilibrium conditions of their decomposition, *Chem. Technol. Fuels Oils* 51 (2015) 470–479, doi:[10.1007/s10553-015-0627-4](https://doi.org/10.1007/s10553-015-0627-4).
- [6] K. Nasrifar, J. Javanmardi, A. Rasoolzadeh, A. Shoushtari, Experimental and Modeling of Methane + Propane Double Hydrates, *J. Chem. Eng. Data.* 67 (2022) 2760–2766, doi:[10.1021/acs.jced.2c00243](https://doi.org/10.1021/acs.jced.2c00243).
- [7] J.L. Thakore, G.D. Holder, Solid vapor azeotropes in hydrate-forming systems, *Ind. Eng. Chem. Res.* 26 (1987) 462–469, doi:[10.1021/ie00063a011](https://doi.org/10.1021/ie00063a011).
- [8] Y. Seo, S.-P. Kang, J. Lee, J. Seol, H. Lee, Hydrate equilibrium data of the CH<sub>4</sub> + C<sub>3</sub>H<sub>8</sub> gas mixture and simulated natural gas in the presence of 2,2-dimethylbutane and methylcyclohexane, *J. Chem. Eng. Data.* 56 (2011) 2316–2321, doi:[10.1021/je1012982](https://doi.org/10.1021/je1012982).
- [9] A.P. Semenov, R.I. Mendgaziev, A.S. Stoporev, V.A. Istomin, D.V. Sergeeva, A.G. Ogienko, V.A. Vinokurov, The pursuit of a more powerful thermodynamic hydrate inhibitor than methanol. Dimethyl sulfoxide as a case study, *Chem. Eng. J.* (2021) 130227, doi:[10.1016/j.ccej.2021.130227](https://doi.org/10.1016/j.ccej.2021.130227).
- [10] V.P. Melnikov, A.N. Nesterov, A.M. Reshetnikov, A.G. Zavodovsky, Evidence of liquid water formation during methane hydrates dissociation below the ice point, *Chem. Eng. Sci.* 64 (2009) 1160–1166, doi:[10.1016/j.ces.2008.10.067](https://doi.org/10.1016/j.ces.2008.10.067).
- [11] A.P. Semenov, R.I. Mendgaziev, T.B. Tulegenov, A.S. Stoporev, Analysis of the techniques for measuring the equilibrium conditions of gas hydrates formation, *Chem. Technol. Fuels Oils* 58 (2022) 628–636, doi:[10.1007/s10553-022-01429-w](https://doi.org/10.1007/s10553-022-01429-w).
- [12] A.P. Semenov, Y. Gong, V.I. Medvedev, A.S. Stoporev, V.A. Istomin, V.A. Vinokurov, T. Li, New insights into methane hydrate inhibition with blends of vinyl lactam polymer and methanol, monoethylene glycol, or diethylene glycol as hybrid inhibitors, *Chem. Eng. Sci.* 268 (2023) 118387, doi:[10.1016/j.ces.2022.118387](https://doi.org/10.1016/j.ces.2022.118387).
- [13] A.P. Semenov, Y. Gong, V.I. Medvedev, A.S. Stoporev, V.A. Istomin, V.A. Vinokurov, T. Li, Dataset for the new insights into methane hydrate inhibition with blends of vinyl lactam polymer and methanol, monoethylene glycol, or diethylene glycol as hybrid inhibitors, *Data Br.* 46 (2023) 108892, doi:[10.1016/j.dib.2023.108892](https://doi.org/10.1016/j.dib.2023.108892).
- [14] M.B. Yarakhmedov, A.P. Semenov, A.S. Stoporev, Effect of lower alcohols on the formation of methane hydrate at temperatures below the ice melting point, *Chem. Technol. Fuels Oils* (2023), doi:[10.1007/s10553-023-01476-x](https://doi.org/10.1007/s10553-023-01476-x).
- [15] A.P. Semenov, R.I. Mendgaziev, A.S. Stoporev, V.A. Istomin, D.V. Sergeeva, T.B. Tulegenov, V.A. Vinokurov, Dimethyl sulfoxide as a novel thermodynamic inhibitor of carbon dioxide hydrate formation, *Chem. Eng. Sci.* 255 (2022) 117670, doi:[10.1016/j.ces.2022.117670](https://doi.org/10.1016/j.ces.2022.117670).
- [16] A.P. Semenov, R.I. Mendgaziev, A.S. Stoporev, V.A. Istomin, D.V. Sergeeva, T.B. Tulegenov, V.A. Vinokurov, Dataset for the dimethyl sulfoxide as a novel thermodynamic inhibitor of carbon dioxide hydrate formation, *Data Br.* 42 (2022) 108289, doi:[10.1016/j.dib.2022.108289](https://doi.org/10.1016/j.dib.2022.108289).
- [17] K. Röttger, A. Endriss, J. Ihringer, S. Doyle, W.F. Kuhs, Lattice constants and thermal expansion of H<sub>2</sub>O and D<sub>2</sub>O ice Ih between 10 and 265 K, *Acta Crystallogr. Sect. B* 50 (1994) 644–648, doi:[10.1107/S0108768194004933](https://doi.org/10.1107/S0108768194004933).
- [18] S. Swaminathan, B.M. Craven, R.K. McMullan, The crystal structure and molecular thermal motion of urea at 12, 60 and 123 K from neutron diffraction, *Acta Crystallogr. Sect. B* 40 (1984) 300–306, doi:[10.1107/S0108768184002135](https://doi.org/10.1107/S0108768184002135).
- [19] K.C. Hester, Z. Huo, A.L. Ballard, C.A. Koh, K.T. Miller, E.D. Sloan, Thermal expansivity for sI and sII clathrate hydrates, *J. Phys. Chem. B.* 111 (2007) 8830–8835, doi:[10.1021/jp0715880](https://doi.org/10.1021/jp0715880).